REFERENCES

[1] E. L. Ginzton, *Microwave Measurements*. New York: McGraw-Hill, 1957.

[2] S. F. Adam, *Microwave Theory and Applications*. Englewood Cliffs, NJ: Prentice-Hall, 1969.

[3] A. Khanna and Y. Garrault, "Determination of loaded, unloaded, and external quality factors of a dielectric resonator coupled to a microstrip line," *IEEE Trans. Microwave Theory Tech.*, vol. MTT-31, pp. 261–264, Mar. 1983.

[4] C. G. Montgomery, R. H. Dicke, and E. M. Purcell, *Principles of Microwave Circuits*. New York: Dover, 1965.

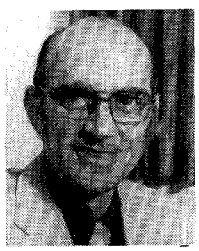

Darko Kajfez (SM'67) was born in Delnice, Yugoslavia, in 1928. He received the Dipl. Ing. degree in electrical engineering from the University of Ljubljana, Yugoslavia in 1953, and the Ph.D. degree from the University of California, Berkeley, in 1967.

Between 1950 and 1963, he worked with companies "Iskra" and "Rudi Cajavec" in Yugoslavia, primarily in the areas of microwave radios and radars. From 1963 to 1966, he was a research assistant at the Electronics Research Lab., University of California, Berkeley, investigating spiral and helical antennas for circular polarization, and their feeding circuits. In 1967, he joined the University of Mississippi, University, where he is presently Professor of Electrical Engineering. During the academic year 1976/77, he was a Visiting Professor at the School of Electrical Engineering, Ljubljana, Yugoslavia. His research and teaching interests are in the areas of electromagnetic theory and its applications to microwave circuits and antennas.

Eugene J. Hwan (S'65–M'65) received the Engineer's degree in 1960 from the Bandung Institute of Technology, Indonesia, and the M.S. degree in electrical engineering in 1966 from the University of California, Berkeley.

From 1960 to 1964, he worked at Siemens and Halske, Munich, Germany, in the field of communication systems. He was a Research Assistant at the Electronics Research Laboratory, University of California from 1965 to 1966. In 1966, he joined Aertech Industries working on microwave components and subsystems. Since 1973, he has been with the Farinon Division, Harris Corporation, where his responsibilities include development of frequency modulated oscillators, low-noise oscillators, and subsystems.

A Nonlinear Analysis of the Effects of Transient Electromagnetic Fields on Excitable Membranes

PAOLO BERNARDI, SENIOR MEMBER IEEE, AND GUGLIELMO D' INZEO, MEMBER, IEEE

Abstract—**The transmembrane voltage produced by a transient electromagnetic field has been determined using a nonlinear model of the cellular membrane. The influence on the membrane voltage of the various parameters characterizing the incident field, such as wave-shape, time-width, and amplitude, has been analyzed. In particular, the amplitude of the incident field for which the cell's behavior can be assumed as linear and the threshold level for exciting action potentials on the membrane have been determined. Potential hazards for humans exposed to transient fields are examined in light of this interaction mechanism.**

I. INTRODUCTION

THE EVALUATION of hazardous levels of nonionizing RF and microwave (MW) radiations requires a deep knowledge of the interaction mechanisms between electromagnetic (EM) fields and biological systems.

Manuscript received June 29, 1983; revised February 6, 1984.

The authors are with the Department of Electronics, University of Rome "La Sapienza," Italy.

The so-called thermal effect, produced by the energy dissipated within the tissue, has been, until now, the most examined one [1], [2]. Since the thermal effect is usually not influenced too much by the temporal behavior of the absorbed EM field, the major part of the literature on the subject is devoted to interactions produced by harmonic fields.

A nonthermal interaction mechanism, considered more recently [3]–[6], consists of the displacement of the membrane voltage from its resting value produced by the field acting at the cellular membrane level. This mechanism is strongly influenced by the temporal dependence of the field absorbed within the tissue. Therefore, it is important to analyze the effects produced on the membrane by EM fields having a general temporal behavior.

Mac Gregor [3], studying a linear model of the interaction process, has shown that a CW incident plane-wave with a frequency of 100 MHz and amplitude 200 V/m

0018-9480/84/0700-0670$01.00 ©1984 IEEE

(corresponding to a power density of 100 W/m^2) can produce alterations of tenths of a millivolt on the transmembrane potential. He also estimated that more remarkable effects can be induced by modulated fields having the same mean power density. However, we observe that, for these latter fields, a linear model of the cell membrane cannot be considered adequate.

Barnes and Hu [4] adopt a nonlinear model of the membrane and assume an exponential current-potential law which approximates the steady-state $I-V$ characteristic of a squid axon membrane. Their results, therefore, can be considered valid only under temporal stationary conditions. Moreover, in their quantitative analysis, the transmembrane dc current variations induced by an incident field are calculated through a square-law approximation, so the treatment gives acceptable results only for incident fields inducing sufficiently small signals across the membrane.

Cain [5] studies the effects on excitable cellular membranes, adopting the Hodgkin and Huxley (H. H.) nonlinear model [7]. He assumes that the incident ac field has a frequency sufficiently high to prevent the ionic channel conductances from following its temporal behavior. Therefore, his analysis considers only the effects produced by steady-state (dc) variations of the abovementioned conductances.

None of the cited works analyses the nonlinear response of the membrane to transient incident fields.

Since, as is shown by H. H. equations [7], the membrane behavior is nonlinear and nonstationary, in this work, we analyze in detail the problem of the response of a membrane exposed to an incident field having an arbitrary temporal behavior. This analysis appears important for various reasons. Firstly, high-amplitude impulsive fields can simulate real exposure situations [8], such as electromagnetic pulse (EMP) simulators, radar transmitters, or electromagnetic compatible systems. Moreover, impulsive fields seem to produce greater biological effects than those induced by harmonic fields having the same mean power density [3]–[5]. In this paper, we analyze in particular the influence on the membrane of the various parameters characterizing a transient incident field, such as the waveshape, the amplitude, and the time-width. The analysis allows us to examine whether the exposure levels adopted by the safety standards, generally based on limiting thermal effects, can be considered satisfactory, in light of this type of interaction mechanism.

II. Description of the Methodology

In order to study the response of a cellular membrane to a transient incident field, the interaction process is subdivided into two parts: a) a linear macroscopic model is adopted to relate the absorbed EM field and the induced current density to the incident field, and b) the effects produced on the membrane potential by the current density induced in the tissue are evaluated using the H. H. nonlinear model. This procedure allows the determination of the temporal behavior of the voltage induced on a cell membrane embedded into a tissue irradiated from fields having a general time-dependence.

A. Interaction at a Macroscopic Level

The determination of the distribution of the absorbed field into a biological body exposed to harmonic fields has been carried out in the past for various exposure conditions and for different geometrical models. Models with a geometrical shape suitable for simulating the human body under free-space irradiation conditions have been considered extensively [9]. Analyses of absorption in realistic near-field exposures and models irradiated in proximity to the ground-plane or other scattering objects also have been developed [10]–[13]. In the works cited, the research has been conducted through: 1) The electrical characterization of the tissue at a macroscopic level, assuming as constitutive parameters a frequency dispersive complex dielectric constant and a magnetic permeability equal to that of the vacuum, and 2) The choice of geometrical models suitable for simulating the exposed subject in the actual exposure conditions. Models similar to those of the exposed bodies or organs (sphere, cylinder, prolate spheroid) are principally used at frequencies up to about 30 MHz; at higher frequencies, in the microwave range, more simple models (semi-infinite plane, plane slab) are usually adopted.

Exposures to EM fields having an arbitrary temporal dependence have been studied using simpler models [8], [14]. Lin [8] studied the problem of a plane-wave Gaussian pulse normally incident on a semi-infinite layer model characterized by a complex dielectric constant having a frequency dependence described by a single Debye relaxation term. Guy [14] examined a plane-wave impulsive field incident on a sphere of muscle-type material whose constitutive parameters are frequency independent.

In this work, a more accurate model is used, both for the dispersion law of the complex dielectric constant and for the simulation of the exposed subject. This is important because, in choosing the model, one must take into account the fact that typical nonharmonic EM fields, to which a subject can be exposed, are mainly of the following two types:

1) Microwave fields modulated with a train of rectangular pulses of short width (normally a few microseconds) and with a repetition rate of some milliseconds, and

2) Transient fields of short width (typical values range from 10 ns to 100 μs) with a nonrepetitive behavior, as a rule.

In the first case, the frequency spectrum of the field is narrow and close to the microwave carrier-frequency; in the second, the spectrum extends along a large band from zero up to a few hundreds of a megahertz.

In order to study, in a quantitative simple way, the interaction of such a large variety of transient fields, it has been necessary to simulate both the dispersive behavior of the dielectric constant and the geometry of the exposed subject on a frequency band as large as possible.

In previous works [12], [15], the authors have shown that, calculating the dielectric constant for a muscular tissue

TABLE I

MUSCLE TISSUE WITH HIGH WATER CONTENT

$\epsilon_\infty = 22.49$ $\sigma_0 = 0.25$ (S/m)

$\alpha_1 = 2.19\times10^6$ $\tau_1 = 1.62\times10^{-3}$ sec
$\alpha_2 = 7.61\times10^4$ $\tau_2 = 3.74\times10^{-6}$ "
$\alpha_3 = 7.44\times10^3$ $\tau_3 = 3.03\times10^{-7}$ "
$\alpha_4 = 85.6$ $\tau_4 = 3.72\times10^{-9}$ "
$\alpha_5 = 9.08$ $\tau_5 = 1.21\times10^{-10}$ "
$\alpha_6 = 22.7$ $\tau_6 = 9.24\times10^{-12}$ "

FREQ.	ϵ' LITERATURE	ϵ' COMPUTED	ϵ'' LITERATURE	ϵ'' COMPUTED
10 Hz	-	2.25×10^6	-	450 $\times10^6$
20 "	2.5×10^6	2.19×10^6	186 ÷434 $\times10^6$	225 $\times10^6$
100 "	1 $\times10^6$	1.16×10^6	20.4 -44.6$\times10^6$	46.0 $\times10^6$
200 "	500 $\times10^3$	509 $\times10^3$	-	23.3 $\times10^6$
1 kHz	130 $\times10^3$	105 $\times10^3$	$2.16\div4.55\times10^6$	4.71×10^6
2 "	99 $\times10^3$	88.8 $\times10^3$	-	2.36×10^6
10 "	70 $\times10^3$	79.9 $\times10^3$	236 ÷480 $\times10^3$	488 $\times10^3$
20 "	60 $\times10^3$	70.0 $\times10^3$	290 $\times10^3$	265 $\times10^3$
100 "	20 $\times10^3$	19.0 $\times10^3$	74 ÷104 $\times10^3$	75.9 $\times10^3$
200 "	10 $\times10^3$	9.93$\times10^3$	42 $\times10^3$	41.5 $\times10^3$
1 MHz	2 $\times10^3$	1.89×10^3	7.8 ÷11 $\times10^3$	11.0 $\times10^3$
2 "	650	654	5.2 $\times10^3$	5.80×10^3
10 "	160	157	1.2 $\times10^3$	1.20×10^3
20 "	127	130	540 ÷600	625
100 "	68	67.7	106 ÷160	150
200 "	58	57.9	85 ÷115	78.4
1 GHz	51	51.0	23 -30	21.2
3 "	46	46.0	13	12.3
5 "	44	44.0	14	11.4
10 "	40	39.6	15	12.6

with only one Debye term, the experimental values of the real and imaginary parts of the complex dielectric constant can be approximated only in a frequency range of about a decade. If, on the contrary, the frequency-dependent complex dielectric properties of the biological tissue are modeled by a frequency-independent static conductivity σ_0, an infinite frequency limit permittivity ϵ_∞, and a number N of Debye relaxation terms, as follows:

$$\epsilon_c(\omega) = \epsilon'(\omega) - j\epsilon''(\omega) = \frac{\sigma_0}{j\omega\epsilon_0} + \epsilon_\infty + \sum_{n=1}^{N} \frac{\alpha_n}{1 + j\omega\tau_n} \tag{1}$$

where each of the nth summation terms corresponds to a relaxation time τ_n, the experimental behavior of the complex dielectric constant can be approximated in a wider frequency range.

Adopting (1) we can determine, through an optimization technique, the values of the parameters $\sigma_0, \epsilon_\infty, \alpha_n, \tau_n$, and the number of terms necessary to fit with good approximation, in the 10-Hz–10-GHz frequency range, the experimental values given in the literature for the dielectric constant of a high water-content tissue. Table I reports the parameter values allowing an approximation better than 20 percent in the whole frequency range; as can be seen, six relaxation terms are necessary. In the following part of the work, a dielectric constant given by (1) with the parameters shown in Table I has been assumed.

In order to calculate the absorbed field in an exposed subject, we consider a plane-wave incident field, linearly polarized, propagating in the positive z-direction and having an arbitrary time dependence. This incident field $e_x^i(z,t)$ is representable by a space-temporal law of the following type:

$$e_x^i(z,t) = e_x^i(t - z/c) \tag{2}$$

where c is the velocity of light.

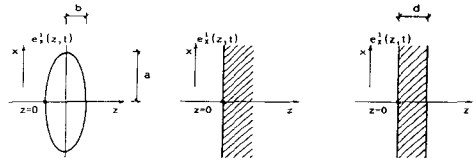

Fig. 1. Geometrical models for the evaluation of the air-body transfer function: 1) Prolate spheroid ($a = 87.5$ cm; $b = 13.8$ cm), 2) Semi-infinite space, 3) Plane layer ($d = 27.6$ cm).

To calculate the time dependence of the absorbed field, three successive steps are necessary: the evaluation of the Fourier transform $E_x^i(z,\omega)$ of the incident field, the calculation of the steady-state transfer function between absorbed and incident field, and the inverse transformation of the absorbed field expression. It is necessary, therefore, to evaluate the transfer function for the geometrical model considered. For a subject having an arbitrary geometrical shape, the transfer function depends on the coordinates and is not representable in a scalar form. Considering the three geometrical models shown in Fig. 1, the transfer function has been calculated as the ratio between the electric field absorbed inside the tissue and the incident field, both evaluated at the interface ($z = 0$ point for the prolate spheroid)

$$T(\omega) = E_x^i(0,\omega)/E_x^i(0,\omega). \tag{3}$$

The absorbed field has been evaluated at the interface because at this point it reaches its maximum.

In order to evaluate the transfer function of the three models of Fig. 1, the field absorbed into the tissue has been calculated through the exact formulation for the two planar models (semispace and slab), while for the prolate spheroid, the long-wavelength approximation [16], [17] has been adopted. The real and imaginary parts of the three transfer functions so obtained are shown in Figs. 2 and 3, respectively.

As can be seen, the three models give quite different results. Since it is known [17] that the long-wavelength approximation gives accurate results, for a man-size spheroid, up to about 30 MHz, the transfer function of the prolate spheroid represents the best approximation in this frequency range. For frequencies higher than 300 MHz, the long-wavelength approximation is no longer applicable, while the results obtained through plane models are sufficiently realistic. In order to represent, with only one analytical expression, the transfer functions of the three models shown in Fig. 1, we adopt the following numerical interpolating formula:

$$T_a(\omega) = T_{aR}(\omega) + jT_{aJ}(\omega) = \sum_{n=1}^{N} \frac{j\omega\beta_n}{1 + j\omega\theta_n} \tag{4}$$

where β_n and θ_n are frequency-independent constants.

Adopting (4), we have determined the values of the parameters β_n, θ_n, and N, giving the least differences from

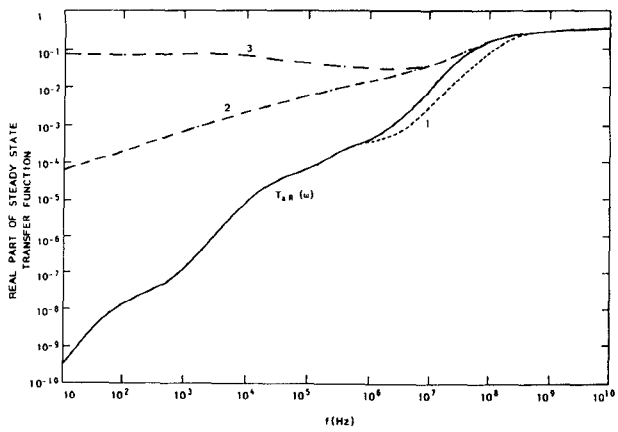

Fig. 2. Comparison between the real parts of the transfer functions of the three models shown in Fig. 1, and that of the interpolation formula $T_{aR}(\omega)$.

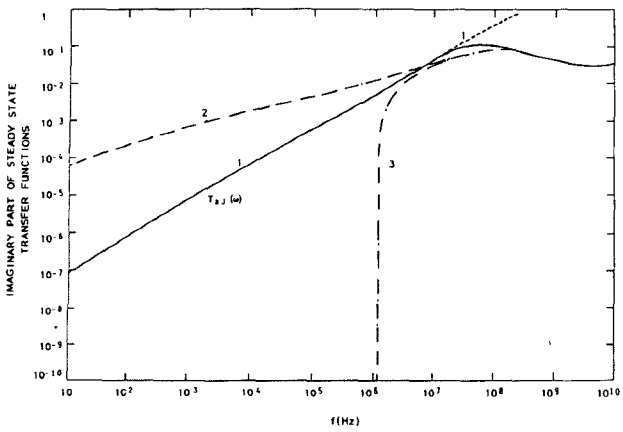

Fig. 3. Comparison between the imaginary parts of the transfer functions of the three models shown in Fig. 1, and that of the interpolation formula $T_{aJ}(\omega)$.

TABLE II
PARAMETERS OF THE INTERPOLATION FORMULA $T_a(\omega)$ (4) WITH $N = 7$. VALUES GIVEN IN SECONDS

$\beta_1 = 4.08 \times 10^{-11}$	$\theta_1 = 1.69 \times 10^{-3}$
$\beta_2 = 3.62 \times 10^{-10}$	$\theta_2 = 6.42 \times 10^{-6}$
$\beta_3 = 1.52 \times 10^{-10}$	$\theta_3 = 4.43 \times 10^{-7}$
$\beta_4 = 7.10 \times 10^{-10}$	$\theta_4 = 3.20 \times 10^{-9}$
$\beta_5 = 2.10 \times 10^{-11}$	$\theta_5 = 4.50 \times 10^{-10}$
$\beta_6 = 3.52 \times 10^{-12}$	$\theta_6 = 1.17 \times 10^{-10}$
$\beta_7 = 5.04 \times 10^{-13}$	$\theta_7 = 5.54 \times 10^{-12}$

the values of the three transfer functions in the frequency ranges in which the models are considered valid. The values obtained are shown in Table II, and the curves $T_{aR}(\omega)$ and $T_{aJ}(\omega)$ also are drawn in Figs. 2 and 3.

After having obtained the numerical expression of (4), and determined the field at the maximum absorption point ($z = 0$) in the frequency domain, the temporal dependence of the absorbed field can be calculated by an inverse Fourier transform. The evaluation of the temporal behavior of the current density induced in the tissue can be obtained in the same manner by an inverse Fourier transform of the steady-state current-density $J(\omega)$, calculated by using (1) and (4).

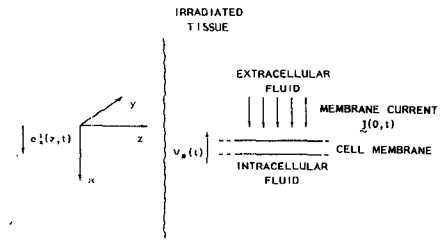

Fig. 4. Model of excitation of the cell membrane. The irradiated tissue zone represents a magnification around the $z = 0$ point of the geometries shown in Fig. 1.

$$\boldsymbol{J}(0,\omega) = j\omega\epsilon_0\epsilon_c(\omega)T_a(\omega)E_x^i(0,\omega)\boldsymbol{x}_0. \tag{5}$$

B. Interaction at a Microscopic Level

The study of the effects of the incident field on the transmembrane potential is carried out adopting the H. H. model to simulate the membrane behavior and considering the current-density induced into the tissue as the cause of excitation of the cell membrane. To adopt the H. H. model, we consider the membrane as a planar structure formed of two parallel surfaces perpendicular to the lines of the current-density and suppose the current-density crossing the membrane to be uniform (Fig. 4). Under such conditions, the surfaces of the membrane are equipotential and a transmembrane potential can be defined. We assume as positive the outside-to-inside potential and positive the current when entering the cell. The outside to inside direction is supposed to be oriented as the x-positive axis

$$\boldsymbol{J}(0,t) = I(t)\boldsymbol{x}_0. \tag{6}$$

Using the model of Fig. 4, the membrane potential $V_m(t)$ can be related to the excitation current $I(t)$ through H. H. equations

$$C_m\frac{dV_m}{dt} + \bar{g}_k n^4(V_m - V_k) + \bar{g}_{Na}m^3h(V_m - V_{Na}) + \bar{g}_l(V_m - V_l) = I(t) \tag{7}$$

$$\frac{d\xi}{dt} = \alpha_\xi(1-\xi) - \beta_\xi\xi, \qquad \xi = m, n, h, \text{ respectively.} \tag{8}$$

In these equations, $V_m(t)$ is the displacement of the membrane potential from its resting value, produced by the current $I(t)$.

Constants C_m, $\bar{g}_k$, $\bar{g}_{Na}$, $\bar{g}_l$, V_k, V_{Na}, and V_l are given in [7], together with the expression of α_ξ and β_ξ, which are functions of the instantaneous value of the membrane voltage $V_m(t)$.

Equations (7) and (8) allow us to obtain the voltage $V_m(t)$ as a function of the current $I(t)$ considered as the known excitation (current clamp condition [18]). The solution of such equations can be carried out numerically using the classical Runge-Kutta method [19].

III. Membrane Response to a Current Excitation

Before studying the effects at membrane level of an impulsive field incident on a biological body, it is useful to analyze the response to a current $I(t)$ directly applied to the membrane. In this way, it is possible to determine the influence on the membrane potential $V_m(t)$ of the various parameters in (7) and (8) and, particularly, of the amplitude and waveshape of the exciting current $I(t)$.

A kind of excitation which allows an accurate study of the membrane behavior, both during the transient and at the steady-state is

$$I(t) = I_0 \sin(2\pi f t)\, u_{-1}(t) \tag{9}$$

where $u_{-1}(t)$ is the Heaviside function.

Some solutions of (7) and (8), corresponding to the current excitation given in (9), are shown in Figs. 5–7. Each of these figures shows the responses corresponding to the same frequency (100 Hz, 1 kHz, and 10 kHz, respectively) and to four different values of the current-density amplitude I_0.

Fig. 5 ($f = 100$ Hz) shows that, for $I_0 = 1\ \mu A/cm^2$, the membrane potential follows the sinusoidal behavior of the exciting current. For $I_0 = 4\ \mu A/cm^2$, the membrane potential is still periodic, but differs from a sinusoidal behavior; moreover, its mean value $\langle V_m(t)\rangle$, computed after a sufficiently high number of periods, begins to assume an appreciable value ($\langle V_m(t)\rangle = -0.24$ mV). For $I_0 = 5\ \mu A/cm^2$ (case c)) the membrane potential differs completely from the previous case—it is always periodic with the same period of the current $I(t)$, but reaches very high values, ten times greater than those obtained for $I_0 = 4\ \mu A/cm^2$.

A further increase in the current amplitude (case d)), $I_0 = 10\ \mu A/cm^2$), produces a behavior of the voltage $V_m(t)$ similar to case c). Case d) shows peaks whose amplitude and period are scarcely influenced by the value of I_0; the only influence of the I_0 increase results in the anticipation of the peaks.

Fig. 6 ($f = 1$ kHz) shows the membrane responses to applied current-density amplitudes of 10, 40, 50, and 100 $\mu A/cm^2$, respectively. In this case also, the membrane behaves nearly linearly for $I_0 = 10\ \mu A/cm^2$, while for $I_0 = 40\ \mu A/cm^2$, its mean value is quite appreciable. If I_0 is greater than 50 $\mu A/cm^2$, peaks of the membrane voltage are excited. Similar to the lower frequency case of Fig. 5, the peaks' amplitude is little influenced by I_0 amplitude once a threshold value is reached; however, it can be noted that the period of the peaks does not correspond to the period of the exciting current, but to a lower period. In particular, the peak repetition rate increases as the current-density amplitude increases (the period of the peaks being equal to about 7 ms in Fig. 6(c) and 4 ms in Fig. 6(d)).

Fig. 7 corresponds to $f = 10$ kHz and $I_0 = 100$, 400, 500, and 1000 $\mu A/cm^2$. The curves show that, in such cases, peaks of the membrane voltage are not excited, so that its behavior, a short time after the current application, is nearly sinusoidal with the same frequency of the exciting

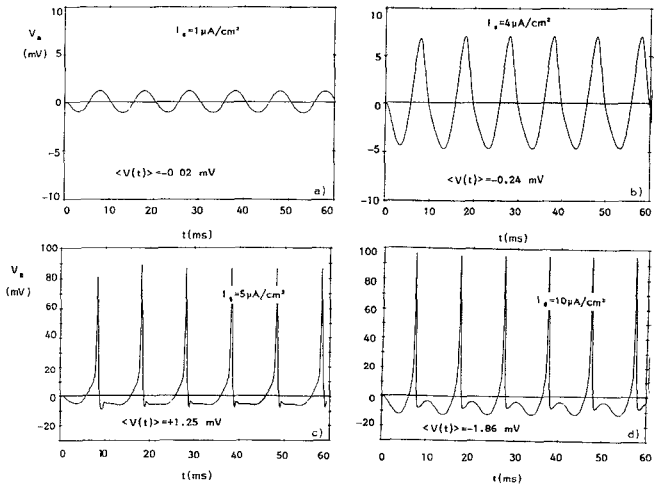

Fig. 5. Membrane responses to four different values of the exciting current-density amplitude I_0; $f = 100$ Hz.

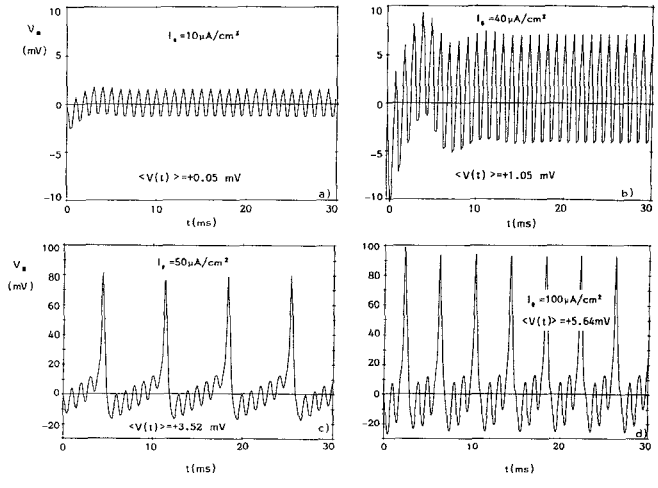

Fig. 6. Membrane responses to four different values of the exciting current-density amplitude I_0; $f = 1$ kHz.

current. It can be noted that, for the first two cases (curves *a*) and *b*)), the mean value of the membrane potential is nearly zero.

The results shown in Figs. 5–7 can be explained on the basis of the following considerations. For the lower frequency case (Fig. 5, $f = 100$ Hz) the membrane potential is essentially influenced by the nonlinear conductances of the sodium and potassium ionic channels [7] whose values suddenly change once a threshold of about 10–15 mV is reached. If the exciting current amplitude I_0 is sufficiently high, this threshold is reached at each cycle, Na^+ channels open, K^+ channels also open, and voltage peaks (action potentials) are produced. Increasing the frequency (Fig. 6, $f = 1$ kHz), the membrane capacitance C_m is not charged at each cycle up to the threshold value, but only partially charged. So, more cycles of the exciting current are necessary in order to reach the threshold. The peaks' repetition rate decreases with increasing I_0, because the membrane capacitance charges more rapidly and reaches the threshold value more quickly. Finally, at $f = 10$ kHz (Fig. 7) the capacitance C_m does not allow the peaks'

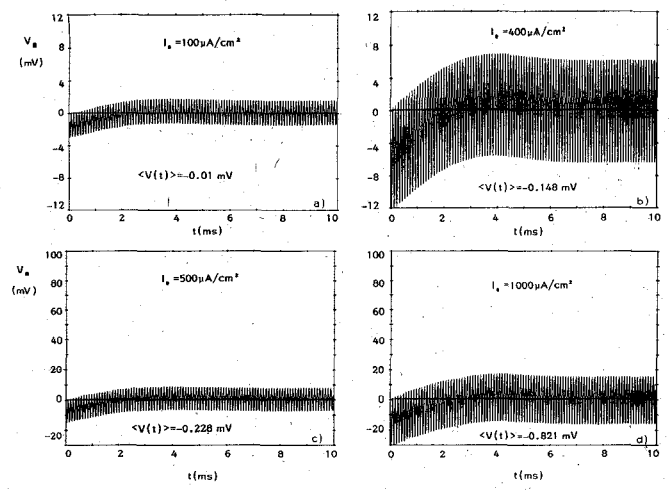

Fig. 7. Membrane responses to four different values of the exciting current-density amplitude I_0; $f = 10$ kHz.

excitation and the membrane nonlinearities are essentially of a quadratic type, producing a mean value of $V_m(t)$ not equal to zero.

From Figs. 5–7, we can note that, when the induced transmembrane voltage reaches amplitudes in the range of 5–10 mV, there is a dc displacement of the outside-to-inside voltage of about 1 mV; while, when the amplitudes are under 1 mV, the cell behavior is nearly linear. In the linear region, the membrane potential follows the behavior of the exciting current $I(t)$, after a short time.

An analysis similar to that discussed in Figs. 5–7 has been repeated by varying the frequency of the current $I(t)$ over the range 10 Hz–100 kHz; Fig. 8 summarizes the results obtained. In this figure, the curve of the current-density amplitude for which the transmembrane voltage reaches 1 mV is shown; below this curve, the behavior of the membrane can be considered as practically linear. In the same figure, the curve giving the I_0 values necessary to excite action potentials on the membrane is also shown; above this curve, therefore, the currents are always sufficient to produce action potentials.

IV. Membrane Effects due to Impulsive Fields

Through the method described in Section II, the temporal dependence of the transmembrane voltage yielded by an impulsive field incident on an exposed body can be evaluated. The case of a plane, linearly polarized, Gaussian pulse of the form

$$e_x^i(z,t) = e_x^i(0,0)\exp\left[-(t - z/c)^2/2t_1^2\right] \qquad (10)$$

where $e_x^i(0,0)$ is the pulse amplitude and t_1 the pulsewidth in time, is considered. Curves of the current-density $I(t)$ induced into the tissue at the point of maximum absorption ($z = 0$) are given in Fig. 9 for Gaussian pulses of amplitude of 1 V/m and pulsewidths of 0.1 μs, 10 μs, and 1 ms.

It can be noted that the shape of the induced current greatly differs from that of the incident field; in particular, the average of $I(t)$ is about zero and its sign changes when the incident pulse reaches approximately its maximum.

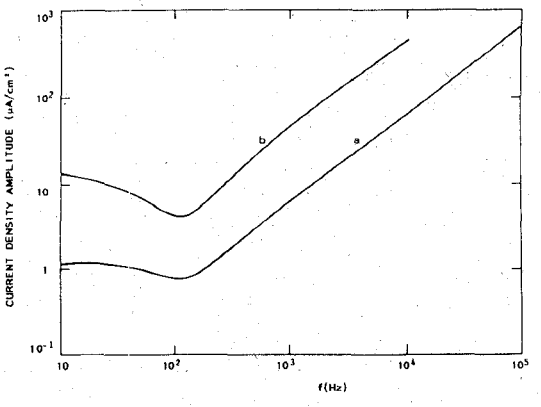

Fig. 8. Current-density crossing the membrane producing: an amplitude of $V_m(t)$ equal to 1 mV (curve a); excitation of action potentials (curve b).

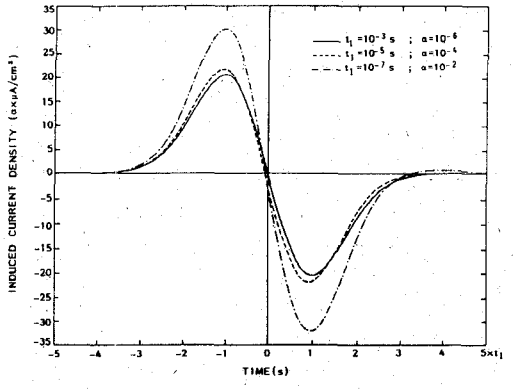

Fig. 9. Induced current density at the maximum absorption point for incident Gaussian pulses of amplitude 1 V/m and width t_1.

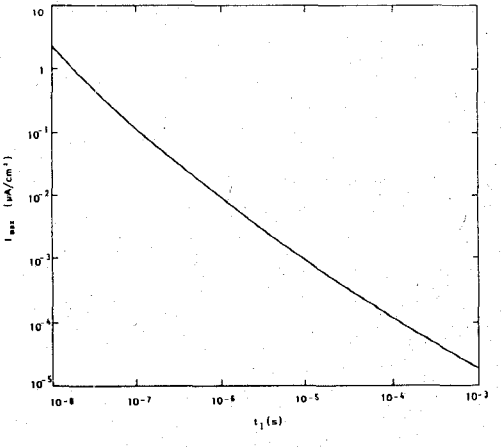

Fig. 10. Maximum value of the induced current density as a function of the time-width of the pulse. $E_0 = 1$ V/m.

Such behavior, already reported in literature [8], [20], [21], is due to the fact that the incident electric field, being always of the same sign, contains a significant component at zero frequency which is totally reflected at the air-body interface, as the transfer function expression (4) shows. The curves of Fig. 9 also show that the amplitude of the current is related inversely to the time-width of the pulse.

In Fig. 10, such behavior is examined in detail, showing the maxima of the induced current as a function of the Gaussian pulse-width (the incident pulse amplitude is nor-

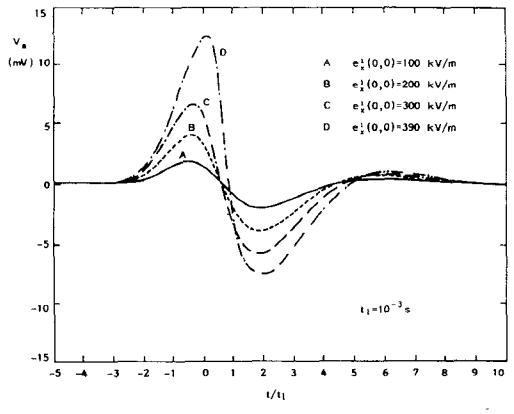

(a)

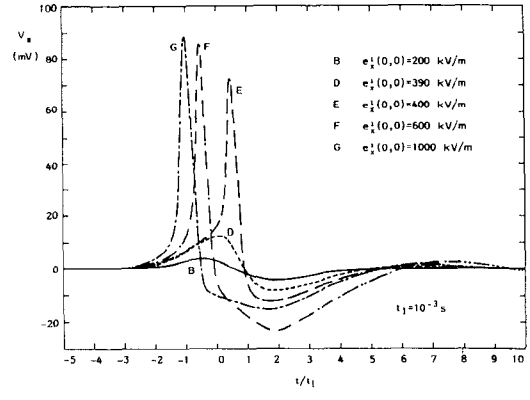

(b)

Fig. 11. Membrane potentials induced by incident plane-wave Gaussian pulses of the form (10); $t_1 = 1$ ms.

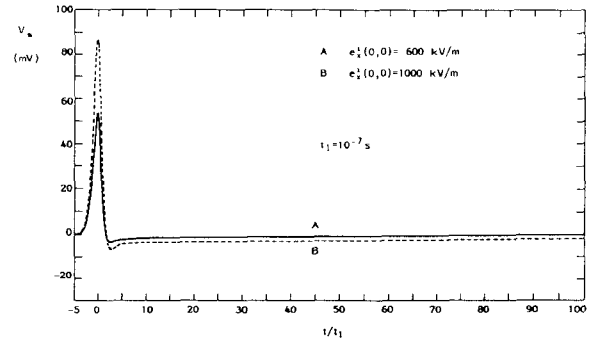

Fig. 12. Membrane potentials induced by incident plane-wave Gaussian pulses of the form (10); $t_1 = 0.1$ μs.

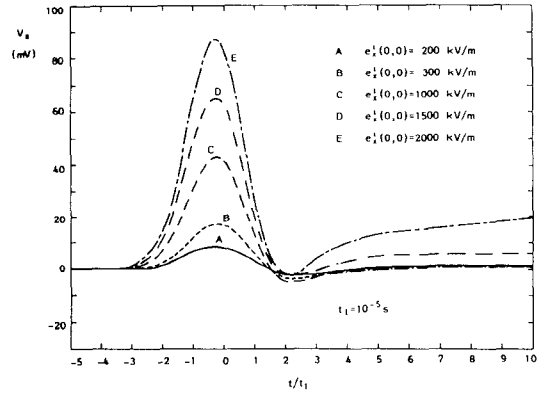

(a)

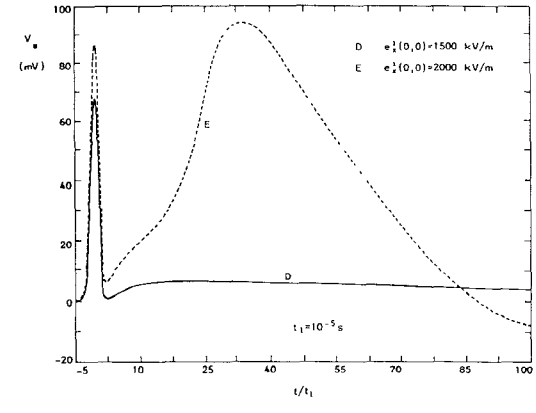

(b)

Fig. 13. Membrane potentials induced by incident plane-wave Gaussian pulses of the form (10); $t_1 = 10$ μs.

malized to 1 V/m). The results of Figs. 9 and 10 are due to the fact that the shorter pulses contain higher spectral components which are more readily absorbed into the tissue.

After having obtained the values of $I(t)$, (7) and (8) have been used in order to obtain the transmembrane voltage $V_m(t)$. Figs. 11 and 12 show the temporal dependence of $V_m(t)$ produced by Gaussian pulses of different amplitudes having pulse-widths $t_1 = 1$ ms and $t_1 = 0.1$ μs, respectively.

Fig. 11(a) ($t_1 = 1$ ms) shows that the transmembrane voltage grows about proportionally to the amplitude of the incident pulse up to values of about 300 kV/m, while a pulse of amplitude equal to 400 kV/m (Fig. 11(b), curve E) excites an action potential on the membrane. Further increasing the amplitude $e_x^i(0,0)$, the voltage peaks have a maximum value approximatively constant, but are excited in advance (curves F, G).

Fig. 12 ($t_1 = 0.1$ μs) shows that increasing $e_x^i(0,0)$ the amplitude of $V_m(t)$ increases too; however, even if the membrane voltage reaches values analogous to that of Fig. 11, there is no action potential excitation.

The temporal dependences shown in Figs. 11 and 12 emphasize a greatly different membrane behavior according to the two excitations considered.

In the first case ($t_1 = 1$ ms, Fig. 11), the excitation $I(t)$ of the membrane is sufficiently slow to allow the ionic component of the membrane current to follow the exciting current variation so that, once $V_m(t)$ has reached the threshold value, ionic channels can open and an action potential is generated. In the second case ($t_1 = 0.1$ μs, Fig. 12), considering the rapid change of the exciting current, the behavior of the transmembrane voltage depends essentially on the capacitive component of the membrane current. Since $I(t)$ changes sign during the pulse and its mean value is about zero, the membrane capacity C_m rapidly charges and discharges, giving rise to the temporal behavior shown in Fig. 12. It can be noted that, even in this case,

$V_m(t)$ reaches values comparable with those of Fig. 11; however, the membrane potential changes much too quickly to allow the opening of the ionic channels.

In Fig. 13, finally, the case of Gaussian pulses having a timewidth intermediate between the previous two ($t_1 = 10$ μs) is examined. In such a case, for $e_x^i(0,0)$ below 1500 kV/m, the behavior of the transmembrane voltage is analogous to that obtained for the shorter pulse (Fig. 12), i.e., the membrane potential returns to its resting-state value, once the excitation is finished. On the contrary, for an amplitude of the incident field equal to 2000 kV/m, the membrane behaves differently. In fact, once the excitation is over, the transmembrane voltage does not return definitely to the resting-state value, but begins to increase again slowly until, as in the case of Fig. 11, the threshold value is reached and there is an action potential excitation. It can be noted that the time-width of the action potential does not depend on the length of the exciting pulse, but is only related to the ionic channels aperture time.

V. Discussion

The analysis carried out in the previous paragraph allows one to determine quantitatively the transmembrane voltage produced by transient electromagnetic fields incident on an exposed body. From such an analysis, within the limits of the model adopted, we obtain some considerations useful for examining the problem of defining the hazard levels of transient EM radiation.

As it has been shown, the cellular membrane has a linear behavior until the harmonic voltage induced on it has an amplitude lower than 1 mV. In such a zone, therefore, we can conduct, using the model examined, a completely linear analysis of the interaction process and link the amplitude of the incident field with the membrane voltage through only one transfer function. The results of this analysis are reported in Fig. 14, where the amplitude of the membrane voltage produced by a linearly polarized harmonic field (amplitude 200 V/m), is shown at a frequency varying from 10 Hz to 10 GHz. This curve shows that the amplitude of the membrane voltage reaches its maxima values for an incident field in the frequency range 1–30 MHz. For lower frequencies, the electric field is strongly reflected by the tissue, while for higher frequencies, even if the portion of the field absorbed into the tissue is increased, the shunt effect of the membrane's capacity prevails. The values obtained in the range 1–30 MHz are comparable with those obtained in [4], where, considering an incident field of 200 V/m, transmembrane voltages of about 10 μV have been evaluated. It is to be noted, however, that the values in [4] are considered as constant over the entire frequency range of RF and MW fields. From Fig. 14, it also can be deduced that, for obtaining voltages equal to 1 mV on the membrane, a CW incident field of about 20 kV/m in the frequency range 1–30 MHz is necessary, while higher fields can be applied outside this interval. Considering incident fields of greater amplitude, the linear analysis is no longer applicable and the transmembrane voltage must be determined in the time-domain.

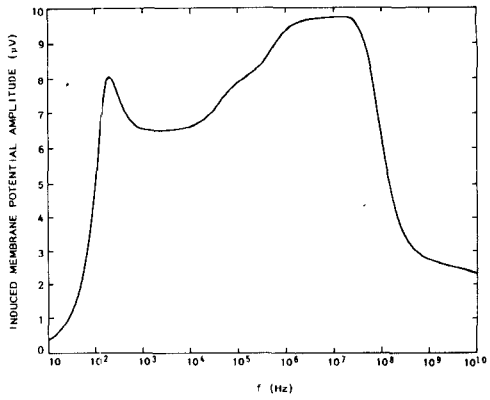

Fig. 14. Amplitude of the membrane voltage induced by a CW, 200 V/m, incident field. Completely linearized analysis.

On the basis of this study, it could be interesting to determine the effects on the membrane produced by an impulsive field verifying the ANSI C 95.1 1974 standard [22]. This standard limits to 100 W/m^2 the time average of the incident power density for any temporal interval of six min. According to this limit, an impulsive EM field having a total energy density $\overline{W}$ equal to 36000 J/m^2 is admissible. Assigning all the abovementioned energy to a single Gaussian pulse, it is possible to calculate the amplitude of such a pulse versus its width t_1

$$e_x^i(0,0) = \left(120\sqrt{\pi}\,\overline{W}/t_1\right)^{1/2}. \tag{11}$$

First, we consider, for example, an incident field of $t_1 = 1$ ms. In such a case, it is obtained from (11) a pulse amplitude equal to 87.5 kV/m. Fig. 15 shows the temporal behaviors of the membrane potential for two values of the incident field, which are, respectively, equal to and greater than that admitted by the cited standard. In the first case, the membrane potential is not sensibly altered in comparison with its resting value, while, in the second case, the incident field produces the excitation of an action potential.

Curves similar to those shown in Fig. 15 can be obtained by varying the time-width t_1 of the incident Gaussian pulse and the results are synthesized in Fig. 16. In this figure, three curves are compared that represent, as a function of t_1, the electric-field amplitudes of a Gaussian pulse for which:

curve *a*) the energy density is equal to the maximum allowed by the 1974 ANSI standard (36 000 J/m^2);

curve *b*) the membrane voltage reaches the value of 1 mV;

curve *c*) action potentials are generated.

The figure shows that the pulse amplitudes admissible on the basis of the ANSI standard do not allow to excite, in any case, action potentials on the cell membrane. Such amplitudes, however, produce voltage displacements from the membrane resting-state value sensibly higher than 1 mV, a level that has been indicated, as a dc voltage, biologically significant [23]. It is necessary, however, to underline that such displacements are of an extremely

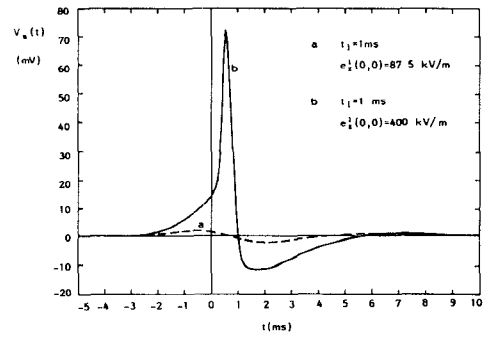

Fig. 15. Temporal behaviors of the membrane voltage produced by a Gaussian pulse: a) $t_1 = 1$ ms; $e_x^i(0,0) = 87.5$ kV/m; b) $t_1 = 1$ ms; $e_x^i(0,0) = 400$ kV/m.

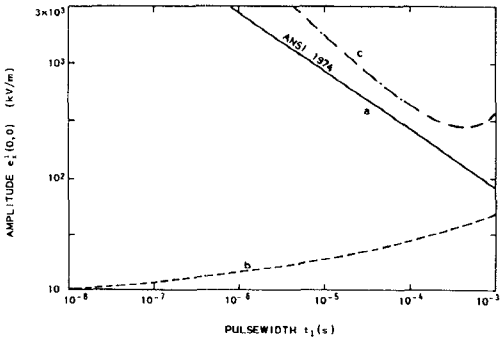

Fig. 16. Amplitude versus width of a Gaussian pulse characterized by: a) constant energy density (36000 J/m^2); b) maximum of the voltage produced on the membrane equal to 1 mV; c) threshold of the excitation of action potentials on the membrane.

short width and that, even today, there are no valid criteria for establishing if effects of this type can assume importance from a biological point of view.

VI. Conclusions

The voltage induced on a cellular membrane by a transient electromagnetic field strongly depends on its temporal characteristics, such as wave-shape, amplitude, and time-width.

For induced voltages lower than 1 mV, the membrane's behavior can be considered as linear. In such a case, the membrane response, as a function of the frequency, shows a maximum in the range 1–30 MHz, where incident fields of about 20 kV/m are necessary to produce 1 mV on the membrane. Above 1 mV, the membrane shows a nonlinear behavior, and a CW incident field can produce a dc voltage on it. A further increase in the amplitude of the incident field can produce action potentials on the membrane.

For impulsive fields, the membrane is particularly sensitive to pulses having a time-width of about 1 ms, i.e., pulse-widths comparable with the proper times of the membrane ionic channels.

The study of the effects produced by impulsive fields satisfying the ANSI C95.1, 1974 Safety Standard has shown that transmembrane voltages greater than 1 mV are produced and that the amplitudes of these voltages are inversely related to the incident pulse-width; however, such pulses can never produce excitation of action potentials.

References

[1] M. A. Stuchly, "Interaction of radiofrequency and microwave radiation with living systems, A review of mechanisms," *Rad. Environm. Biophys.*, vol. 16, pp. 1–14, 1979.

[2] C. Romero-Sierra, "Bioeffects of electromagnetic waves," in *Review of Radio Science 1978–1980*, S. A. Bowhill, Brussels: URSI, 1981, ch. 2.

[3] R. J. MacGregor, "A possible mechanism for the influence of electromagnetic radiation on neuroelectric potentials," *IEEE Trans. Microwave Theory Tech.*, vol. MTT-27, pp. 914–921, Nov. 1979.

[4] F. S. Barnes and C. J. Hu, "Model for some nonthermal effects of radio and microwave fields on biological membranes," *IEEE Trans. Microwave Theory Tech.*, vol. MTT-25, pp. 742–746, Sept. 1977.

[5] C. A. Cain, "A theoretical basis for microwave and RF field effects on excitable cellular membranes," *IEEE Trans. Microwave Theory Tech.*, vol. MTT-28, pp. 142–147, Feb. 1980.

[6] Y. H. Barsoum and W. F. Pickard, "Radio-frequency rectification in electrogenic and nonelectrogenic cells of chara and nitella," *J. Membrane Biol.*, vol. 65, pp. 81–87, 1982.

[7] A. L. Hodgkin and A. F. Huxley, "A quantitative description of membrane current and its application to conduction and excitation in nerve," *J. Physiol.*, vol. 117, pp. 500–544, 1952.

[8] J. C. Lin, "Interaction of electromagnetic transient radiation with biological materials," *IEEE Trans. Electromagn. Compat.*, vol. EMC-17, pp. 93–97, May 1975.

[9] C. H. Durney *et al.*, "Radiofrequency radiation dosimetry handbook (Third edition)," *Report SAM-TR-80-32*, University of Utah, Aug. 1980.

[10] I. Chatterjee, M. J. Hagmann, and O. P.Gandhi, "Electromagnetic energy deposition in an inhomogeneous block model of man for near-field irradiation conditions," *IEEE Trans. Microwave Theory Tech.*, vol. MTT-28, pp. 1452–1459, 1980.

[11] R. J. Spiegel, "The thermal response of a human in the near-zone of a resonant thin-wire antenna," *IEEE Trans. Microwave Theory Tech.*, vol. MTT-30, pp. 177–185, Feb. 1982.

[12] P. Bernardi, G. D'Inzeo, F. Giannini, and R. Sorrentino, "Quantifying the hazard of field-man interaction in electrically shielded enclosures," *Alta Frequenza*, vol. 49, pp. 55–60, 1980.

[13] P. Bernardi, F. Giannini, and R. Sorrentino, "Effects of the surroundings on electromagnetic-power absorption in layered-tissue media," *IEEE Trans. Microwave Theory Tech.*, vol. MTT-24, pp. 621–625, Sept. 1976.

[14] A. W. Guy, "On EMP safety hazards," AGARD Lecture Series no. 78 on Radiation Hazards, 1975.

[15] P. Bernardi, F. Giannini, G. D'Inzeo, and R. Sorrentino, "Electromagnetic power distribution induced in biological tissues in a closed environment," in *Proc. IMPI Microwave Power Symp.*, Monaco, June 1979.

[16] C. H. Durney, C. C. Johnson, and H. Massoudi, "Long-wavelength analysis of plane wave irradiation of a prolate spheroid model of man," *IEEE Trans. Microwave Theory Tech.*, vol. MTT-23, pp. 246–253, Feb. 1975.

[17] C. C. Johnson, C. H. Durney, and H. Massoudi, "Long-wavelength electromagnetic power absorption in prolate spheroidal models of man and animals," *IEEE Trans. Microwave Theory Tech.*, vol. MTT-23, pp. 739–747, Sept. 1975.

[18] R. Fitzhugh, "Thresholds and Plateaus in the Hodgkin-Huxley Nerve Equations," *J. General Physiol.*, vol. 43, pp. 867–896, 1960.

[19] National Physical Laboratory, *Modern Computing Methods*. London: HMSO, 1961.

[20] R. W. P. King and C. W. Harrison Jr., "The transmission of electromagnetic waves and pulses into the earth," *J. Appl. Phys.*, vol. 39, pp. 4444–4452, Aug. 1968.

[21] J. C. Lin, "Electromagnetic pulse interaction with mammalian cranial structures," *IEEE Trans. Biomed. Eng.*, vol. BME-23, pp. 61–65, Jan. 1976.

[22] American National Standard, *Safety Level of Electromagnetic Radiation with Respect to Personnel*, ANSI c. 95.1, 1974.

[23] H. P. Schwan and K. R. Foster, "RF-field interactions with biological systems: Electrical properties and biophysical mechanisms," *Proc. IEEE*, vol. 68, pp. 104–113, Jan. 1980.

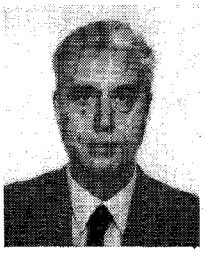

Paolo Bernardi (M'66–SM'73) was born in Civitavecchia, Italy, in 1936. He received the degree in electrical engineering from the University of Roma in 1960 and received the Libera Docenza in Microwaves in 1969.

Since 1961, he has been with the Institute of Electronics of the University of Roma, as Assistant Professor from 1961 to 1965, Associate Professor from 1966 to 1975, Full Professor of Microwave Measurements from 1976 to 1981, and of Microwaves since 1982. His research work has dealt with the propagation of electromagnetic waves in ferrites, microwave components, numerical methods in EM problems, and his present interest is in biological effects of EM waves, particularly on dosimetric and measurements problems.

Dr. Bernardi is a member of AEI and of the NIR Committee of the Italian Radiation Protection Association. He served as Chairman of the IEEE Middle and South Italy Section (1979–80) and as a member of the Editorial Board of IEEE Transactions on Microwave Theory and Techniques. He is a contributor of the Editorial Board of Alta Frequenza, and in March 1980 co-edited a special issue devoted to "Nonionizing electromagnetic radiations." During 1984, he will be awarded with the IEEE Centennial Medal.

Guglielmo d'Inzeo (M'83) was born in Milan, Italy, in 1952. He received the degree in electronic engineering at the University of Rome in 1975.

Upon completion of his studies, he joined the Department of Electronics of the same University, where he has been a Researcher since 1981. From 1979 to 1980, he was a Professor of Electromagnetic Wave Theory and Techniques at the University of Calabria. Since 1979, he has been a Professor of Applied Electronics at the University of Ancona. His research activities are in the fields of microwave components and biological effects of electromagnetic waves.

A Novel *K*-Band Balanced FET Up-Converter

TETSUO HIROTA AND HIROYO OGAWA

Abstract—**The performance of the *K*-band balanced FET up-converter is described. A novel circuit configuration effective in enhancing conversion gain in the FET up-converter is proposed. An analysis using a simplified circuit model shows the effect of LO feedback in the balanced circuit. A conversion gain of 0.9 dB was experimentally obtained at 20 GHz. Maximum output power was 15.9 dBm.**

I. Introduction

GREAT PROGRESS has been made in the GaAs FET from microwave to millimeter-wave frequency ranges. Up until now, high-power and low-noise amplifiers have been developed using FET's. Recently, GaAs FET's are not only being applied to amplifiers, but also to various nonlinear functional circuits, such as frequency converters [1]–[4] and frequency doublers [5]–[7]. The advantages FET's offer are 1) excellent input–output isolation, and 2) desirable output power and gain capability.

The GaAs FET up-converters reported so far have achieved a 0-dB conversion gain at 6 GHz [3] and 8 GHz [4]. The performance of these FET up-converters, however, becomes degraded at *K*-band or higher frequencies due to various parasitic reactance effects.

In this paper, a novel approach to enhance the conversion gain of FET up-converters is proposed. The fundamental characteristics of the FET up-converter are described in Section II. Then, loss-reduction effect gained by LO load optimization is discussed in Section III. The performance of the balanced FET up-converter is presented in Section IV.

II. Frequency Conversion in FET's

Fundamental frequency conversion characteristics of FET's have been experimentally investigated in *K*-band. This investigation includes an examination of the optimum impedance matching conditions and bias points for up-converters. The circuit configuration for an experiment applies both LO power and IF input signal to the gate of source-grounded FET's as shown in Fig. 1. LO and IF signals are mixed by the nonlinear relationship of gate-voltage to drain-current, and the up-converted signal is obtained from the drain. Another approach is to use a dual-gate FET. For up-converter applications, however, a single-gate FET is preferable because it excels in high-frequency performance and the separation of LO and IF is

Manuscript received September 7, 1983; revised February 27, 1984.

The authors are with the Electrical Communication Laboratories, Nippon Telegraph and Telephone Public Corp., 1-2356, Take, Yokosuka-Shi, Kanagawa-Ken 238-03, Japan.

0018-9480/84/0700-0679$01.00 ©1984 IEEE